

1 Using single remote sensing image to calculate the height of the
2 landslide dam and the maximum volume of the lake

3

4 Weijie Zou ^{1,2}, Yi Zhou ¹, Shixin Wang ¹, Futao Wang ¹, Litao Wang ¹, Qing
5 Zhao ¹, Wenliang Liu ¹, Jinfeng Zhu ¹, Yibing Xiong ^{1,2}, Zhenqing Wang ^{1,2},
6 Gang Qin ^{1,2}

7 ¹*Aerospace Information Research Institute, Chinese Academy of Sciences, Beijing, 100094, China;*

8 ²*University of Chinese Academy of Sciences, Beijing 100049, China;*

9 *Correspondence: Yi Zhou (zhouyi@radi.ac.cn) and Futao Wang (wangft@aircas.ac.cn)*

10 **1. Abstract**

11 Landslide dams are caused by landslide materials blocking rivers. After the occurrence of large-scale
12 landslides, it is necessary to conduct large-scale investigation of barrier lakes and rapid risk assessment.
13 Remote sensing is an important means to achieve this goal. However, at present remote sensing is only
14 used for monitoring and extraction of hydrological parameters at present, without prediction on potential
15 hazard of the landslide dam. The key parameters of the barrier dam, such as the dam height and the
16 maximum volume, still need to be obtained based on field investigation, which is time-consuming. Our
17 research proposes a procedure that is able to calculate the height of the landslide dam and the maximum
18 volume of the barrier lake, using single remote sensing image and pre-landslide DEM. The procedure
19 includes four modules: (a) determining the elevation of the lake level, (b) determining the elevation of
20 the bottom of the dam, (c) calculating the highest height of the dam, (d) predicting the lowest crest height
21 of the dam and the maximum volume. Finally, the sensitivity analysis of the parameters during the
22 procedure and the analysis of the influence of different resolution images is carried out. This procedure
23 is mainly demonstrated through Baige Landslide Dam in south-west China. The single image from
24 Beijing-1 and pre-landslide DEM, SRTM V3, are used to predict the height of the dam and the key
25 parameters of the dam break, which are in good agreement with the measured data. And Hongshiyuan
26 landslide dam is also used to validate the procedure. This procedure can effectively support the quick
27 decision-making regarding hazard mitigation.

28

29 **Keywords:** Landslide dam, Remote sensing, DEM, Dam height, Hazard

30 2. Introduction

31 Landslide dams are caused by landslide materials blocking rivers, usually in mountainous areas with
32 rivers and narrow valleys, bringing great risks to local people's lives and property(Costa and Schuster,
33 1988; Fan et al., 2020). Landslide dams disaster is widely distributed around the world. For instance, the
34 11 dams caused by the Magnitude 7.6 earthquake in New Zealand 1929(Adams, 1981); Oso Landslide
35 Dam in Washington, USA in 2014(Iverson et al., 2015); Diexi Landslide Dam on Minjiang River, China,
36 1933(Li et al., 1986); Yigong Landslide Dam in 2000(Zhou et al., 2016) and a series of landslide dams
37 including the Tangjiashan Landslide Dam caused by the Wenchuan earthquake in 2008(Zhang et al.,
38 2019).Based on the historical records of 183 landslide dams, Costa found that the main way of dam
39 breaching was overtopping. 41% of dams breached within one week, and 85% breached within a
40 year(Costa and Schuster, 1988). Respectively Fan analyzed a series of dams induced by the 2008
41 Wenchuan earthquake finding that 43% of them collapsed within one month(Fan et al., 2012). And
42 according to Shen's research on the longevity of the barrier lake, nearly 48.3% of the dams will breach
43 within a week, and 84.4% of the dams will fail within one year(Shen et al., 2020). Most of landslide
44 dams are unstable. However, the landslide dam always occurred in remote mountainous areas, with
45 inconvenient traffic conditions and poor infrastructure(Cui et al., 2009). When earthquakes or
46 precipitation induce large-scale landslides, field survey is time-consuming and manpower-
47 consuming(Dong et al., 2014). Remote areas tend to be more vulnerable and the dam breaching are more
48 likely to cause serious consequences. So, it requires us to identify the landslide dam and take action as
49 quickly as possible.

50
51 There are several factors influencing the process of formation, development and risk of landslide dams.
52 These factors can be divided into three categories. First, the factor of the soil, including the dam material
53 composition and the repose angle of the dam material, has an unavoidable relationship with the formation
54 and erosion process of the dan. The low permeability and high erodibility will lead to short longevity of
55 the landslide dam and fast breaching of the dam(Shen et al., 2020). Second, the hydrological parameters,
56 such as lake volume, average annual discharge and catchment area which decide the speed of lake surface
57 raising(Cao et al., 2011). The faster the lake raises, the less time is left to hazard mitigation. Third, the
58 geometric parameters, such as the length and angle of the landslide surface and the length, width, height
59 of the dam. The landslide surface influences the kinetic energy of the landslide material which has a great
60 influence on the formation of the landslide dam. And the geometric parameters of the dam itself decide
61 the stability of dam, the maximum volume of the lake and the potential maximum discharge of breaching
62 (Dong et al., 2011a; Cao et al., 2011; Shen et al., 2020).

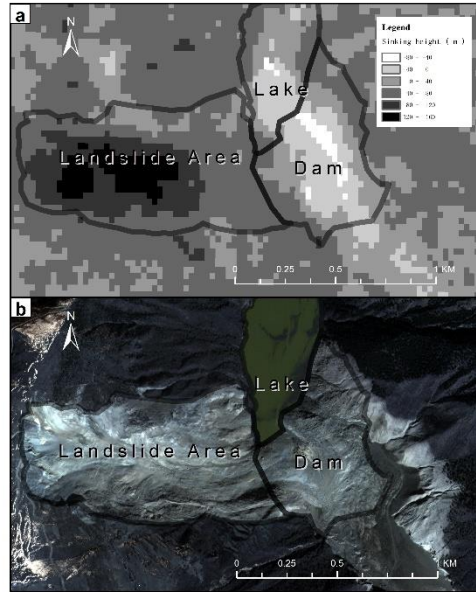
63 Remote sensing has the ability to identify and monitor landslide dams on a large scale conveniently, and
64 supports quick decision-making regarding hazard mitigation(Canutì et al., 2004; Fan et al., 2021). In the
65 research before, remote sensing is usually regarded as an auxiliary means to monitor the change of the
66 catchment area or to measure the length of the dam. For example, Wang and Lv used multiple remote

67 sensing images to extract water boundary images and pre-landslide DEM to monitor the changes of lake
68 volume of Yigong Lake(Wang and Lu, 2002). Respectively, Cheng et al. proposed a method to estimate
69 reservoir capacity of water based on water boundary and DEM(Chen and Lu, 2008).

70 The research above focused on obtaining information of the barrier lake through remote sensing and
71 Geographic Information System. However, these kinds of methods focus on monitoring and can only
72 obtain part of geometry parameters directly through image such as catchment area,Some essential
73 components of hazard evaluation are not available in these research. Especially the height of the dam
74 which determines the maximum volume of the barrier lake and the flood peak of the dam breaching(Costa
75 and Schuster, 1988; Ermini and Casagli, 2003; Peng and Zhang, 2012; Dong et al., 2014) can't be
76 obtained through these methods. However, as most of the landslide dams breach by overtop, they start to
77 breach as long as the elevation of lake surface equals the elevation of the landslide dam(Meng et al.,
78 2021; Costa and Schuster, 1988; Ermini and Casagli, 2003). So, the height of the landslide dam decides
79 the maximum volume of berried lake. The damage of the landslide dam mostly relies on the flood it
80 causes through breaching. As water goes through the dam surface, the erosion process will lead to rapid
81 increase of the discharge and finally result in flood. According to research, his process has a strong
82 relationship with the height of the landslide dam(Anon, 2021; Shen et al., 2020; Chen et al., 2004; Braun
83 et al., 2018), which makes it one of the most important parameters related to this hazard.

84 With the rapid development of Unmanned Aerial Vehicles (UAVs), in 2008, photogrammetric UAVS are
85 also used to survey the landslide dams in the Wenchuan earthquake in 2008(Cui et al., 2009). However,
86 after the earthquake, there are to be a large number of landslides and the affected area is considerably
87 huge. If UAVs are used for precise investigation one by one, it cannot meet the requirements of timeliness
88 for the emergency. Based on the pre-landslide DTM and a series of remote sensing images after the
89 landslide dam, Dong obtains the variation of the lake level to estimate the slope foot of the barrier dam
90 and predict the dam height, completing quickly assessment of the dam breaching hazard(Dong et al.,
91 2014). But this procedure is still inconvenient as it requires sequential images to predict the height of the
92 dam. All of the methods that use the pre-landslide DEM are based on an important assumption that the
93 pre-landslide DEM is reliable. Nevertheless, take Baige Landslide Dam as example (Fig 1), we can find
94 that the elevation of landslide area changes greatly. The landslide area has a greater degree of subsidence,
95 and the dam area has a greater degree of uplift. And even in areas nearby covered with vegetation, there
96 was about 20 meters of subsidence averagely, which demonstrates that the assumption above nee further
97 improvement.

98 This research will focus on the weakness above using single remote sensing image and pre-landslide
99 DEM to obtain the essential information of the landslide dam and calculating the height of the landslide
100 dam based on the formation mechanism of the landslide dam. The Baige Landslide Dam is taken as an
101 example to verify the feasibility of this procedure. And the sensitivity analysis of the parameters during
102 the procedure and the analysis of the influence of different image resolution will be carried out in the
103 discussion part.

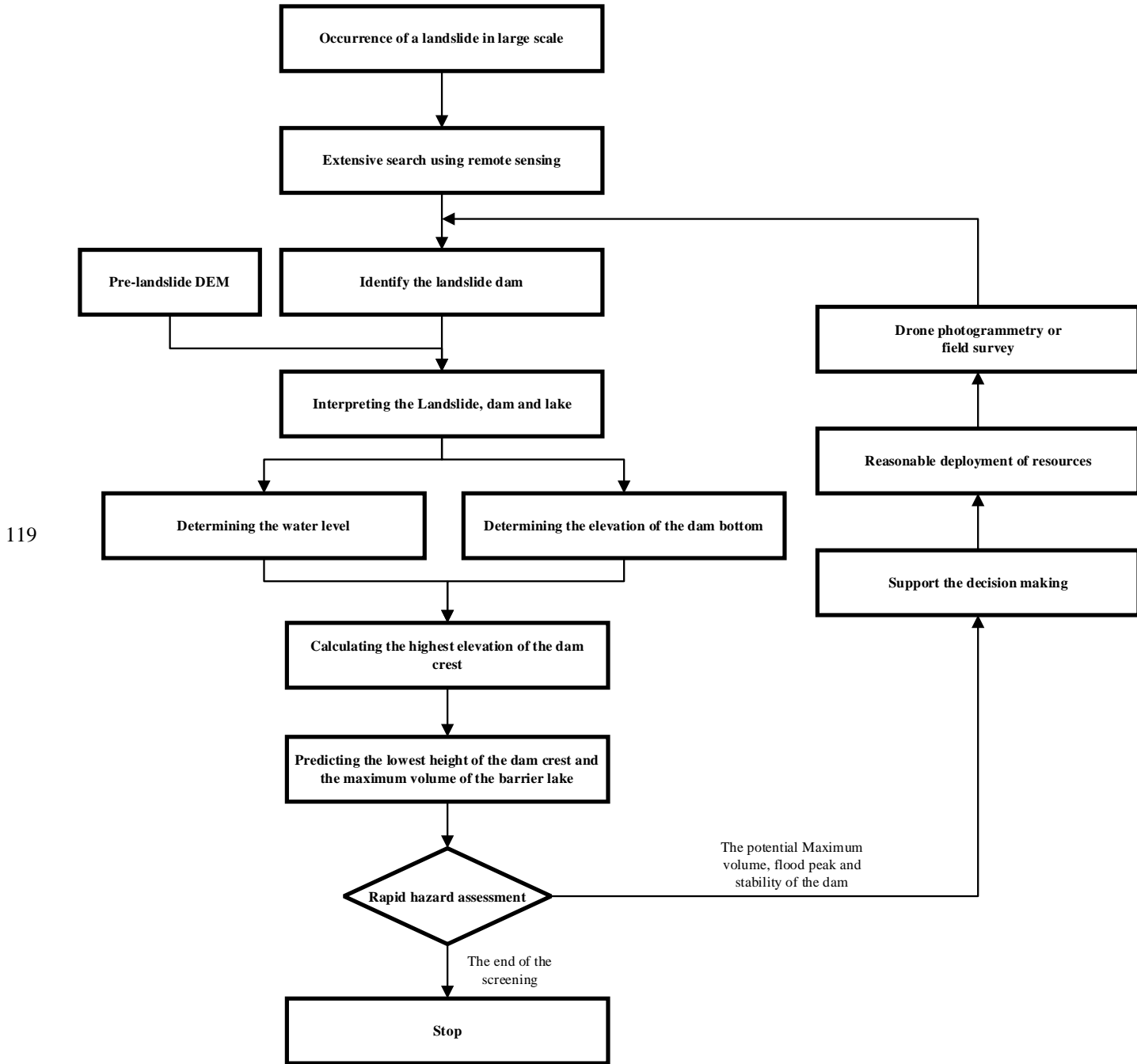


104

105 Fig 1 picture a is the comparison of pre-landslide DEM (SRTM V3) and the after-landslide DEM. And
 106 picture b is the remote sensing image from Beijing-1 satellite (taken in November 9, 2018)

107 3. Procedure

108 After the occurrence of large-scale landslides, the government often can't get all the disaster situation
 109 immediately, so large-scale landslides investigation is needed. As the disaster often occurs in remote
 110 areas, the purpose of the large-scale investigation is not only to find the landslide dams, but also to make
 111 an objective evaluation of the hazard of the landslide dams, supporting reasonable allocation of resources
 112 to avoid excessive reaction. When a landslide dam is identified from the image, the procedure to calculate
 113 its height is divided into four parts: (a) selecting the reference points to determine the elevation of the
 114 lake level; (b) estimating the elevation of the bottom of the dam; (c) calculating the highest elevation of
 115 the dam crest based on the formation mechanism of the landslide dam; (d) predicting the lowest height
 116 of the dam crest and the maximum of the lake volume. This section will elaborate the details of (a), (b),
 117 (c) and (d), obtaining the lowest height of the dam crest and calculating the maximum volume based on
 118 GIS.

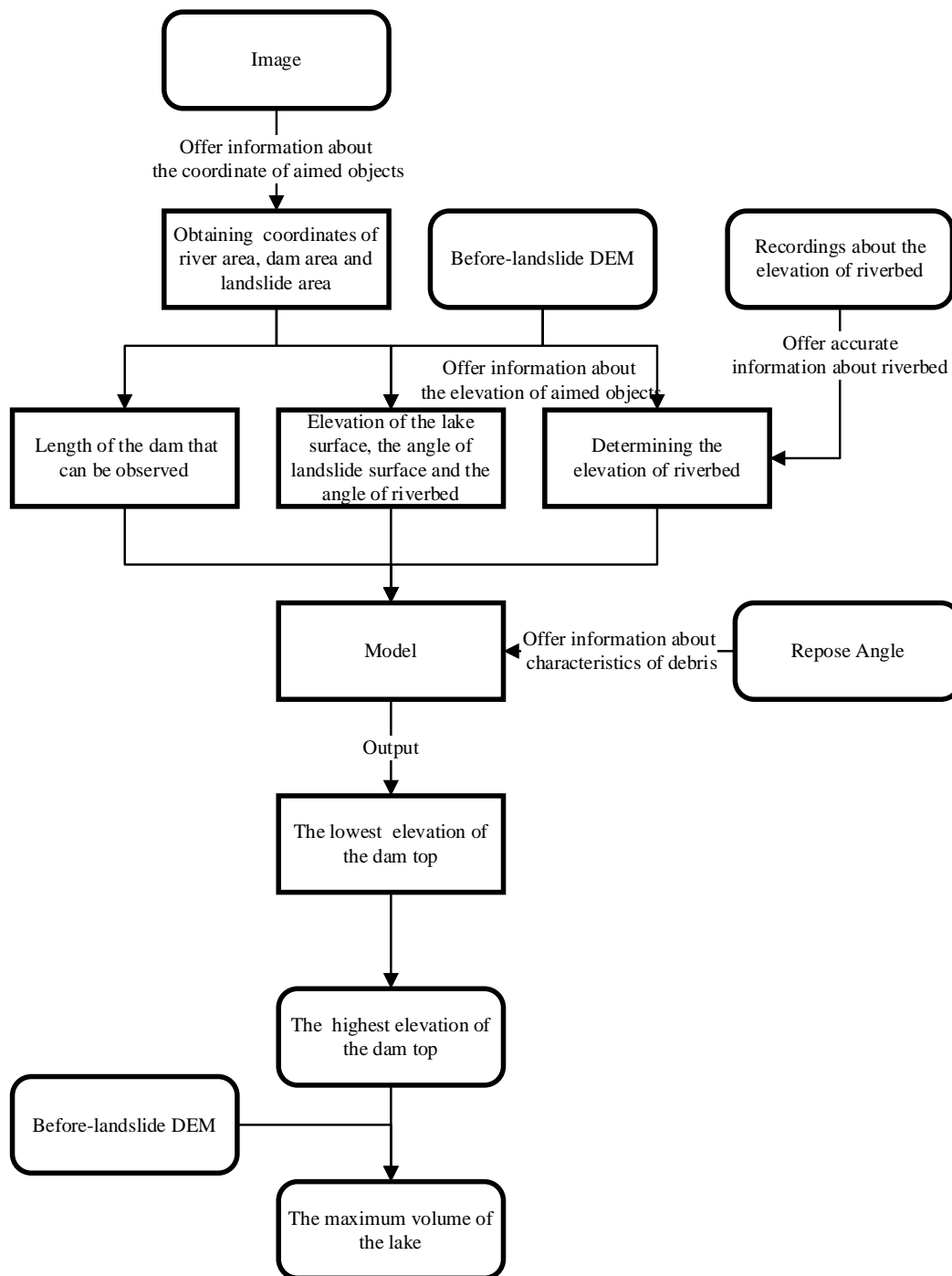


120

121 Fig 2 the procedure of obtaining the height of the dam crest and completing the hazard assessment

122 This study provides a method to predict critical information about a barrier dam using limited real-time
 123 data. The data required includes an after-landslide satellite image and a pre-event DEM. The data that
 124 is not required include the repose angle of the nearby material and the elevation of the riverbed. If there
 125 are reliable recordings, they can be used in the procedure to improve the prediction accuracy.

126 Otherwise, our research provides a reliable method to predict them. The whole prediction of dam
 127 elevation information based on the above input data will be explained in the following sections. The
 128 process of use of each input data, determination of intermediate parameters and final output results is
 129 shown in Fig 3.



130

131 Fig 3 the complete process of determination of parameters in the procedure of prediction

132 3.1. Determining the elevation of the lake level

133 The method of estimating the elevation of the barrier lake based on remote sensing images has been
134 practiced by many scholars. Typically speaking, researchers assume that the elevation of the water
135 boundary is the same as the topography. And pre-landslide DEM is used in most cases to determine the
136 lake level with the water boundary in the image(Wang and Lu, 2002; Chen and Lu, 2008; Dong et al.,
137 2014; Braun et al., 2018). However, the reliability of the pre-landslide DEM may decrease as a result of
138 landslides (Fig 1). The reasons are summarized as follows: (a) the landslide has caused some changes in
139 the topography of the area; (b) the pre-landslide DEM has errors itself, especially in the mountainous
140 area; (c) as the pre-landslide DEM usually can not be undated in time, there can be some landslides
141 without records before.

142 For the reasons above, the selection of the reference points to determine the elevation of the lake level
143 should follow these principles to reduce errors. (a) As landslides often bring about large-scale ground
144 subsidence, when selecting reference points, the point around the landslide area should be avoided. (b)
145 Because landslides and settlements tend to occur in areas with steep terrain and little vegetation
146 coverage(Ayalew and Yamagishi, 2005) and the DEM is more precise in flat terrain, the reference points
147 should be in vegetation-covered flat terrain, avoiding gully or ravines.

148 Under these strictions the reference points selected can be regarded as having the same elevation of the
149 lake level. Therefore, the lake level is determined. However, in order to determine the elevation of the
150 lake level, a complex number of reference points are needed. Their value can't be the same for the random
151 errors but should be within a certain range(Fig 6), for the random errors of DEM and the errors in the
152 process of determining the points. In this situation, points that are one and a half interquartile range away
153 from the mean value are considered outliers. And the elevation of the lake level is the average elevation
154 of the remains. Because the dam blocks the channel and the river has no outflow, the water surface can
155 be assumed to be still(Wang and Lu, 2002; Morgenstern et al., 2021; Fan et al., 2021). So, the elevation
156 of the lake level is the same as the elevation of the dam-lake point in Fig 3.

157 3.2. Determining the elevation of the dam bottom

158 In this procedure, the bottom of the dam refers to the point where the dam meets the river bed on the
159 downstream side. In practical cases, the most reliable method is to directly use the riverbed elevation
160 obtained recently. In the absence of relevant data, the following method should be taken for prediction.

161 Within a certain range, the riverbed elevation can be considered to decrease in proportion along the
162 channel, conforming to a linear variation. Therefore, sampling elevation points at the lowest point of the
163 river valley in the pre-landslide DEM, removing the outliers and carrying out simple regression to obtain
164 the fitting of the riverbed elevation. By extending the fitting results to the dam body and subtracting the
165 historical river depth, the bottom elevation of the dam is obtained.

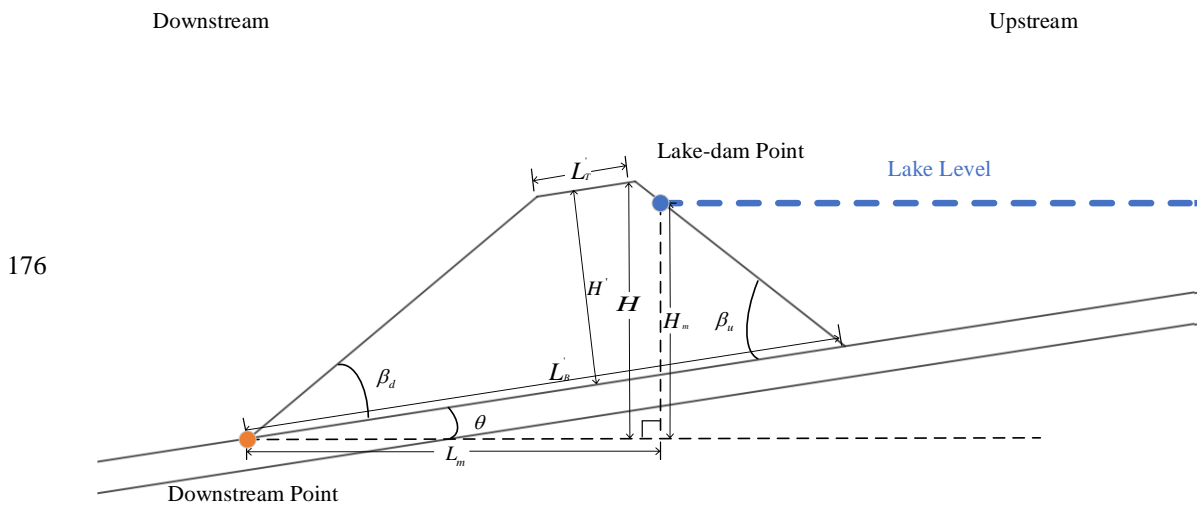
166 However, the historical river depth is to vary with the seasons. So, there must be some errors in this
167 prediction. The influence of dam bottom elevation on calculating dam height will be analyzed in the

168 “discussion” section.

169 3.3. Calculating the highest elevation of the dam crest

170 According to Wu's laboratory experimental study, the geometrical form of the barrier dam is mainly
 171 determined by landslide slope, river slope, angle of repose, earthwork amount and sliding height. I (Wu
 172 et al., 2020).

173 With his theory, if the river is completely blocked and the valley can be simplified into U-shape, the
 174 longitudinal section of the landslide dam can be simplified as a trapezoid(Wu et al., 2020) as shown in
 175 Fig 4. And the trapezoid will follow the following pattern.



177 Fig 4 simplified section of the landslide dam

178 The top of the dam is parallel to the bottom of the dam (Wu et al., 2020).

179 $L'_T \parallel L'_B$ (1)

180 Where L'_T is the top of the dam, L'_B is the bottom of the dam (Wu et al., 2020).

181 $\beta_d + \theta = \beta_u - \theta = \chi\phi$ (2)

182 Where β_d is the angle between the body of the dam and the riverbed on the downstream side, β_u is
 183 the angle between the body of the dam and the riverbed on the upstream side, ϕ is the angle of repose
 184 of the landslide mass and χ is the parameter that fits the effect of “cut top” phenomenon. ϕ is
 185 determined by the nature of the soil itself and χ will be affected by landslide surface angle, landslide
 186 length and other factors(Grasselli et al., 2000). The determining of the χ can be simplified as
 187 follows(Wu et al., 2020):

188 $\chi = 0.57 + 0.51(1 + e^{\frac{(\alpha-34)}{10.50}})^{-1}$ (3)

189 where α is the angle of the landslide surface. As the angle is higher, the actual angle between the
 190 riverbed and the landslide material will be smaller and the length of the dam along the river will be longer.
 191 Normally speaking, this formula fits the actual situation well. The precise of this fitting will be discussed

192 in the “discussion” section.

193 According to Wang's field investigation on the Wenchuan earthquake, it is found that the angle of repose
194 of landslide dam in the Wenchuan earthquake is between 28.8° and 44.7°, with an average of 35.5° (Wang
195 et al., 2013). In the absence of relevant data, it is recommended to use the average provided by Wang.

$$196 \quad \varphi = 35.5^\circ \quad (4)$$

197 Wu proposed that the height of the dam has a certain relationship with the length of the bottom of the
198 dam (Wu et al., 2020), as follows:

$$199 \quad H' = (0.37 + 1.1 \tan \theta) \cdot \tan(\beta_d + \theta) \cdot L_B' \quad (5)$$

200 where H' is the height between the dam top and the dam bottom, θ is the angle of the riverbed and

201 L_B' is the length of the dam along the river. The R^2 of formula (1) (2) (3) (5) are all greater than 0.95.

202 As shown in Fig 3, the elevation of the dam-lake point and the elevation of the dam bottom has already
203 been obtained before. So, H_m can be calculated and L_m can be obtained directly from the remote
204 sensing images. According to formula (1), (2), (3), (4) and (5), using simple geometric relations, the
205 following relation can be obtained:

206

$$207 \quad L_B' = \frac{L_m}{\cos \theta} + \frac{\cos(\beta_u - \theta)}{\sin \beta_u} \cdot (H_m - L_m \cdot \tan \theta) \quad (6)$$

$$208 \quad H_r = \sin \theta \cdot (L_B' - H' \cdot \tan \theta - H' \cdot \tan(90 - \beta_u)) \quad (7)$$

209

$$210 \quad H = \frac{H'}{\cos \theta} + H_r \quad (8)$$

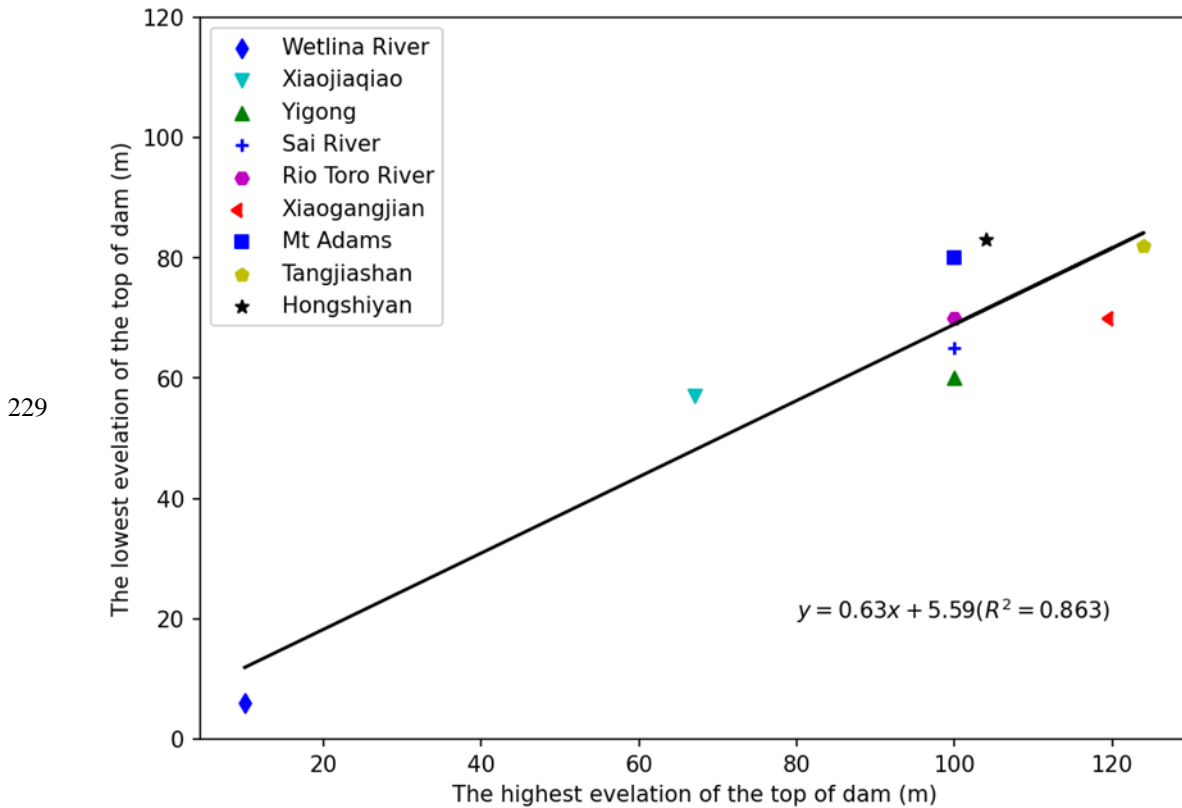
211 Where H is the difference between the highest elevation of the dam crest and the dam bottom
212 elevation and H_r is the difference of the elevation of the riverbed between the dam bottom and the
213 crest. θ and α can be obtained through the remote sensing image and the pre-landslide DEM easily.

214 Through this procedure, the highest elevation of dam crest is determined based on a single image and
215 pre-landslide DEM, which can be used in the further prediction of the dam breaching and related
216 decision-making.

217 3.4. Predicting the lowest height of the dam crest and the 218 maximum volume of the barrier lake

219 Because the height of the landslide dam in the vertical direction of the river channel will not be
220 consistent (Costa and Schuster, 1988; Fan et al., 2020), but will form different types of distribution
221 according to the characteristics of the case, resulting in the height of the landslide dam is not a simple
222 value but a range. As the most important factor affecting the dam breaching is the height of the lowest

223 point of the dam crest, which determines the potential maximum volume of the barrier lake and the
 224 maximum discharge volume of the dam breach(Costa and Schuster, 1988; Chen et al., 2004, 2021; Dong
 225 et al., 2011b, 2014; Yang et al., 2013; Zhong et al., 2018), the prediction result of the highest elevation
 226 of the dam crest can't be used in related breaching models directly.
 227 But by simply analyzing the highest elevation of the dam crest and the lowest elevation in the existing
 228 records, a simple estimation of the relationship between them is carried out, as shown in Fig 5.



230 Fig 5 the relationship between the highest elevation of the dam crest and the lowest elevation of the
 231 dam crest. These datas can be found in the papers of Cui, Costa, Mora and so on(Costa and Schuster,
 232 1991; Mora Castro, 1993; Briaud, 2008; Cui et al., 2009; Peng and Zhang, 2012; Chen et al., 2020).

233 .
 234 The relationship can be expressed as follows:

235
$$H_l = 0.63H_h + 5.59(R^2 = 0.863) \quad (9)$$

236 where H_l is the lowest elevation of the dam crest and H_h is the highest elevation of the dam crest.

237 On the basis of the formula above, we can use this procedure to complete the rapid assessment of the
 238 breaching hazard.

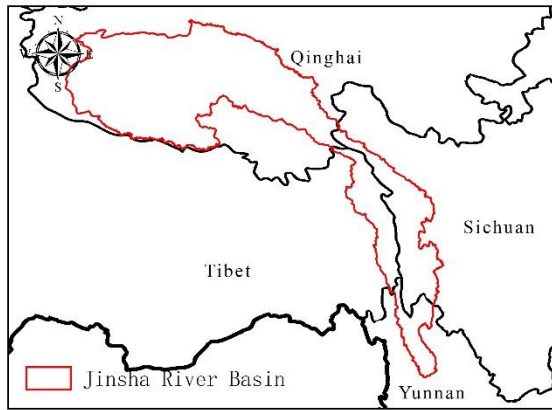
239

240 4. Validation of the proposed procedure

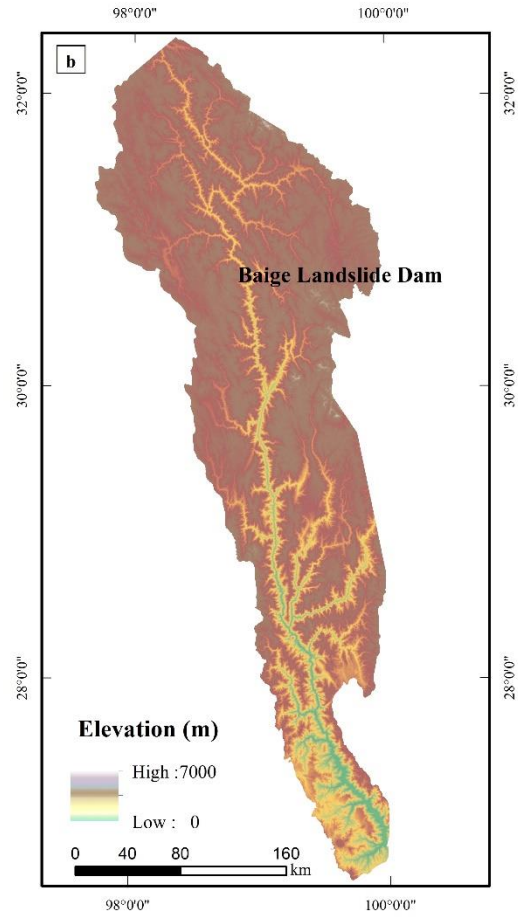
241 4.1. Baige Landslide Dam

242 The Jinsha River, the upper reach of the Yangtze River, was dammed twice recently at Baige, Tibet, one
243 on 10 October 2018 and the other on 3 November 2018 (UTC+8), at $98^{\circ}42'32.24''\text{E}$, $31^{\circ}4'59.27''\text{N}$ (Fig
244 4) (Zhang et al., 2019) and one on November 3, 2018, the residual landslide of "10.10" Baige Landslide
245 Dam slid down again, forming "11.03" Baige Landslide Dam on the basis of the original residual dam(Li
246 et al., 2019). The dam is much larger than the first one, as the width of the dam top is 195 m, the length
247 of the dam top is 273 m and the highest elevation of the dam crest is 3014m(Chen et al., 2020). After
248 proper treatment, its storage capacity is reduced from $8.69 \times 10^8 m^3$ to $5.79 \times 10^8 m^3$ and the flood
249 peak is diminished from $41624 m^3 / s$ to $31000 m^3 / s$ (Chen et al., 2020; Yunjian et al., 2021). A
250 large number of roads and bridges were damaged downstream, and a total of 54,000 people were affected,
251 with economic loss of over 7.43 billion yuan(Zhang et al., 2019). Due to abundant field survey data and
252 its great harm, Baige Landslide Dam was selected to demonstrate this procedure.

253 Baige Landslide Dam occurred in a deep valley of the mountainous area and the barrier lake is long and
254 narrow (Fig 6). To demonstrate the proposed procedure, we take the second Baige landslide as example.
255 The image used is a 0.8m resolution image from Beijing-1 which was taken on November 9, 2018 and
256 the pre-landslide DEM we choose is SRTM V3 of 30m resolution which was taken in 2000. The effect
257 of the resolution of the image will be discussed in the "Discussion" section.



258



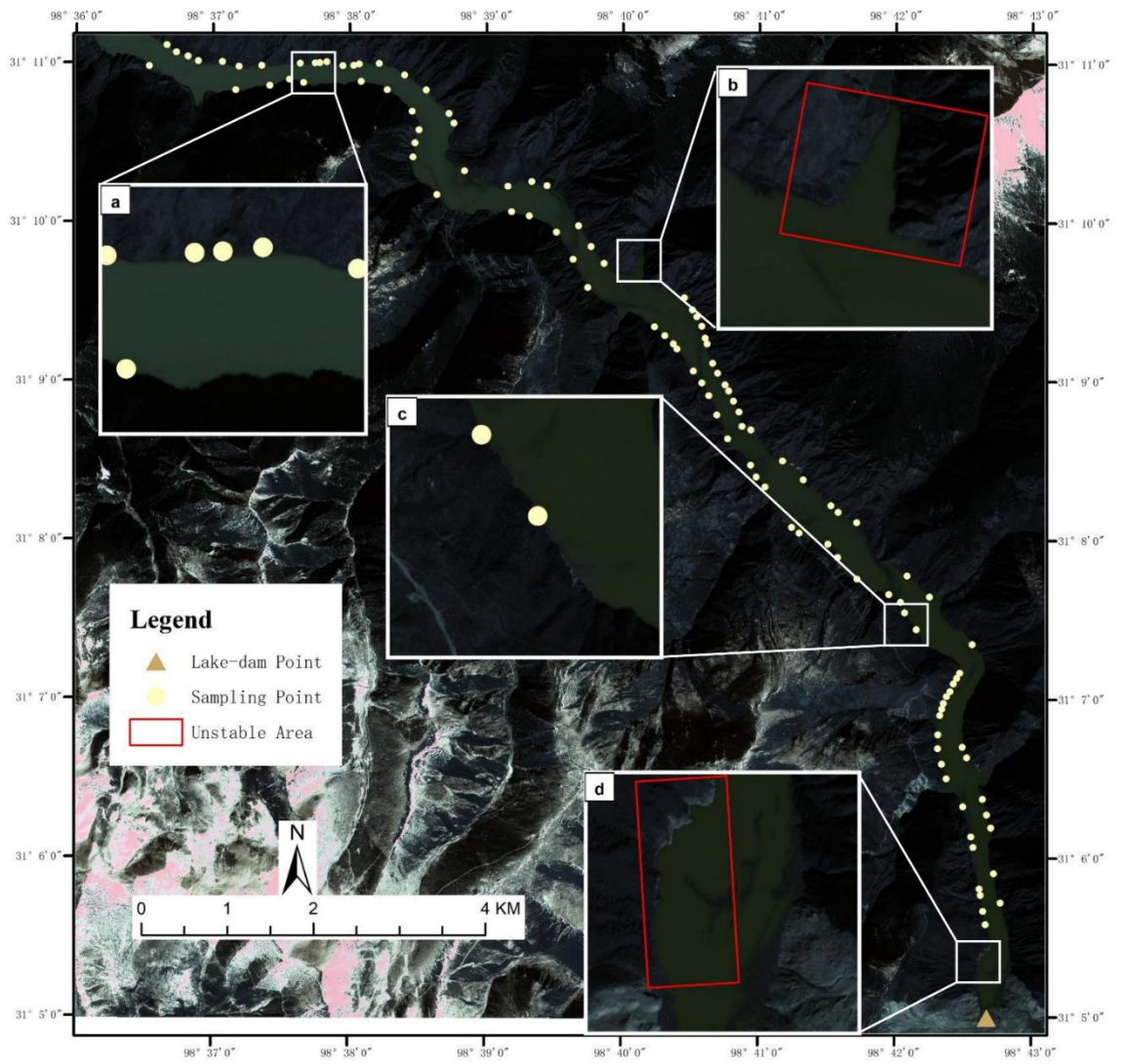
259 Fig 6 the position of the Baige Landslide Dam

260 **4.2. Determine the elevation of the lake level**

261 At the water boundary in the remote sensing image, the area covered by vegetation with relatively flat
 262 terrain and a certain distance from the landslide was selected for elevation sampling (Fig 6). Under ideal
 263 circumstances, the distribution of sampling points' elevation should be completely consistent. But in
 264 practice, there are often large deviations, shown in Fig 8, the specific reasons for which have been
 265 discussed in the "Procedure" section and will not be repeated. The deviation between the maximum and
 266 minimum elevation of sampling points can reach 72m, and the shape basically conforms to the normal
 267 distribution. Therefore, the mean of reference points can be obtained directly after clearing the outliers,
 268 which is the elevation of barrier lake and the outcome is 2944m. Since the lake is essentially still, the
 269 elevation of the lake should be the same as the elevation of the point where the dam meets the lake,
 270 shown as the triangle in Fig 7.

271

272

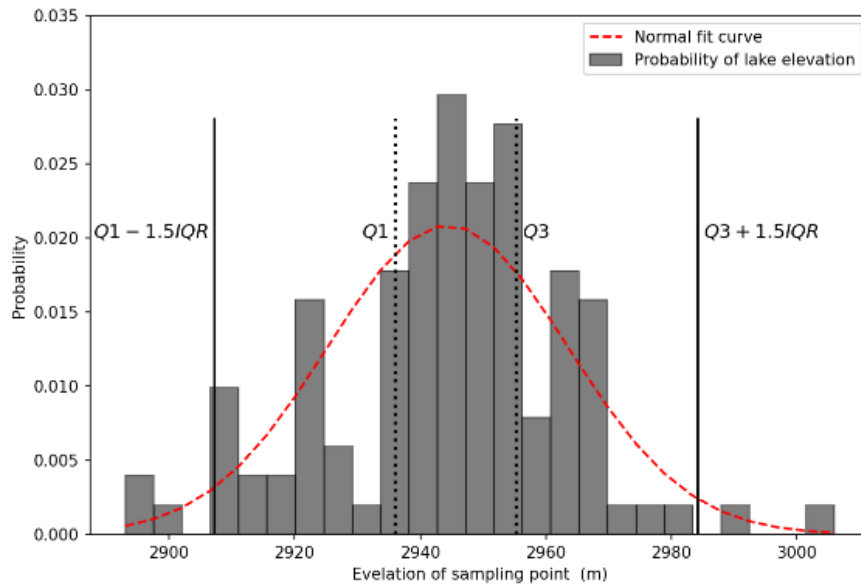


273

274

275 Fig 7 the sampling points in the case of Baige Landslide Dam (image from Beijing-1 satellite)

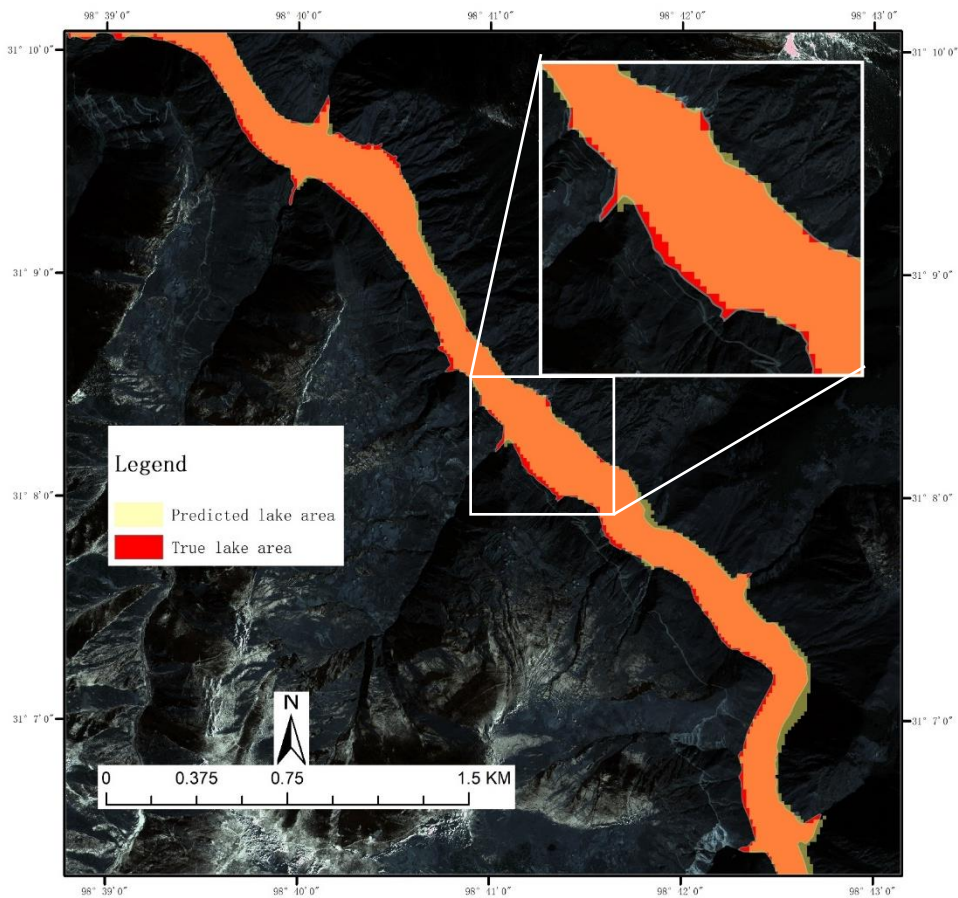
276



277 Fig 8 elevation distribution of sampling points

278 The Intersection over Union (IOU) of the area with elevation below 2944m in DEM and the actual
279 submerged area in the remote sensing image is 84.48% (Fig 9). The two are found to be basically
280 consistent.

281



282 Fig 9 the comparison of the area with elevation below 2944m in DEM and the actual submerged area in

283 the remote sensing image (image from Beijing-1 satellite)

284 4.3. Determining the elevation of the dam bottom

285 The inclination angle of the riverbed is calculated by sampling and unitary regression and is about 0.11° .
286 The elevation of the water level on the place of dam bottom before the landslide is 2867m. As the water
287 depth is not considered when obtaining DEM and varies with change of rainfall in the rainy season and
288 dry season, this value can't be used directly. According to the data in China Ministry of Water Resources
289 Information Center, the water depth of Jinsha River section is about 2-10m. The water depth can be
290 assumed as the mean value, 6m. Therefore, the final estimate of the dam bottom elevation is 2861m.
291 Respectively, according to the field survey, the riverbed elevation is 2860m(Chen et al., 2020).
292

293 4.4. Calculating the highest height of the dam crest

294 The slope angle of the landslide surface, the inclination angle of the riverbed and the length of the
295 landslide can be calculated directly through remote sensing image and DEM. The slope angle of landslide
296 surface is 30.65° . The inclination angle of the riverbed is 0.11° . And the length of the landslide that can
297 be observed is 567m. According to formula (5) (6) (7) (8), with the parameters obtained before, the
298 highest height of the dam top is 155.4m and the highest elevation of the dam top is 3016.5m with an error
299 of 2.5m compared to the measured data by Chen, 3014m(Chen et al., 2020).

300 4.5. Predicting the lowest height of the dam crest and the 301 maximum volume of the barrier lake

302 Taking Baige Landslide Dam as an example, according to the case section, we have predicted that the
303 highest elevation of the dam crest is 3016.5m and the height of the dam is 155.4m. According to formula
304 (9), we calculated that the lowest height of the crest of the landslide dam is 104.2m, and the elevation is
305 2964.2m with an error of 2.8m compared to the measured data by Chen, 2067m(Chen et al., 2020). Using
306 Geographic Information System, we can estimate based on DEM(Wang and Lu, 2002; Chen and Lu,
307 2008) that its potential maximum volume is $7.96 \times 10^8 (m^3)$.

308 4.6. Another case for validation

309 Another case for validation is Hongshiyuan landslide dam, a landslide created by moderate earthquake
310 (Ms 6.5) on August 3rd, 2014. The epicenter of the earthquake is located at 27.11° N, 103.35° E and the

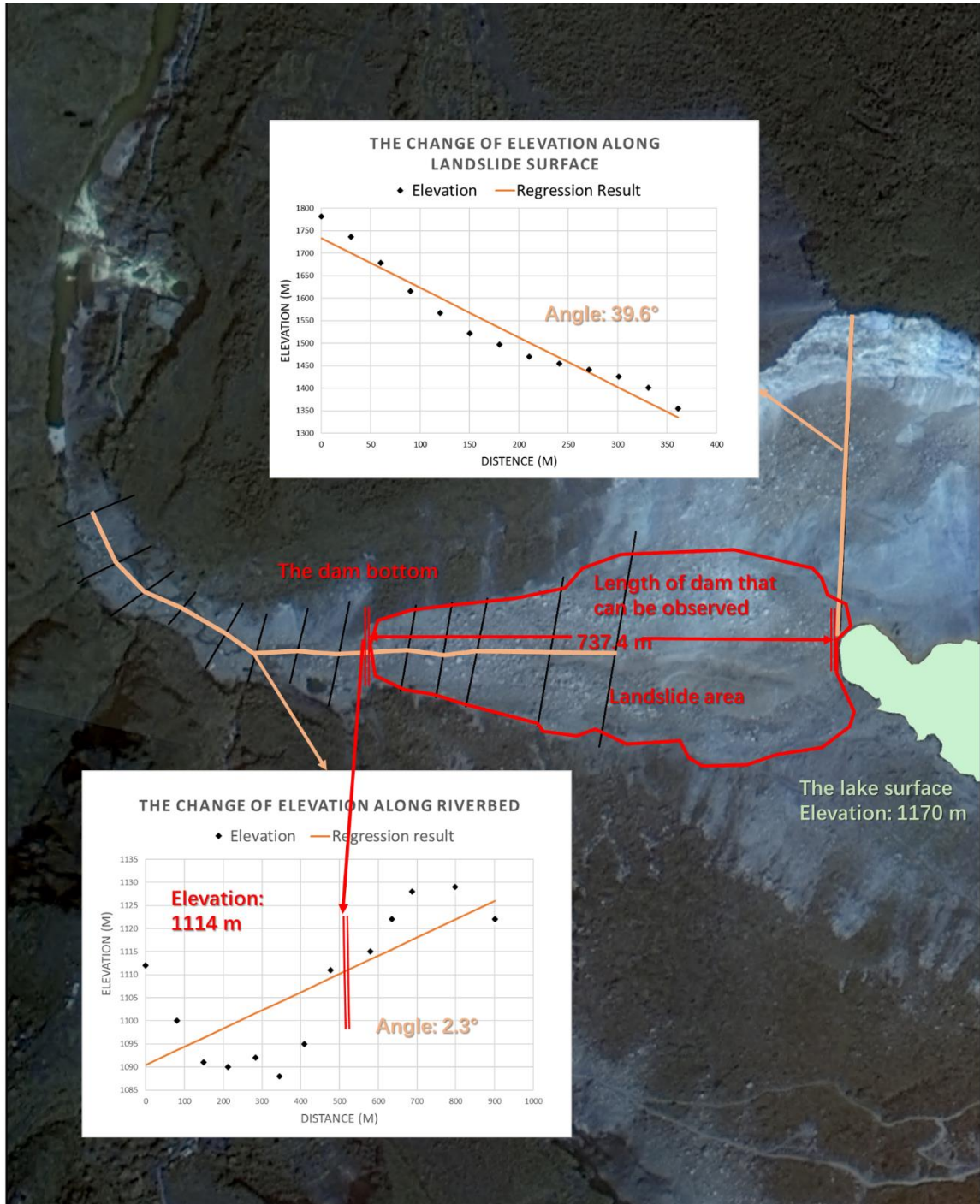
311 landslide is 8.8 km southeast from the epicenter(Luo et al., 2019). The landslide dam is over 78 meters
 312 above the water, holding a maximum water storage of 2.6×10^8 m³(Zhou et al., 2015). Breaching of this
 313 giant dam will not only pose a high threat to the residents who live around, but also bring a possibility to
 314 damage other hydropower dams downstream. The data used to carry out the procedure in this research
 315 and predict the essential geometry parameter of landslide dam is listed in Table 1, including an after-
 316 landslide remote sensing image(2 m solution) and a pre-event DEM.
 317

Input data	Source	Description
After-landslide Remote sensing image	Gaofen-1 satellite	2 m solution
Pre-landslide DEM	SRTM V3	30 m solution
Repose angle of the debris	Relative case recording	Rough estimation
The elevation of riverbed	Sampling from DEM	Rough estimation

318 Table 1 Source of input data used in the Hongshiyuan case.

319 Firstly, the image and the DEM is used to obtain the parameters required to make the prediction. The
 320 elevation of the lake level is obtained by sampling lake edge points. As shown in Fig 10, the elevation of
 321 the water level on the place of dam bottom before the landslide can be obtained through sampling the
 322 lowest points along the riverbed in the DEM (every lowest point in each black line), which is 1114m.
 323 The lake level is 1170 m. As the water depth of Niulan River is about 3 m(Zhou et al., 2015), the elevation
 324 of the dam bottom is 1111m. Therefore, the difference between them, H_m , is 59 m. The length of the
 325 landslide dam that can be observed, L_m , is measured directly in the image, which is 737.4 m (Fig 10).
 326

327



328

329

Fig 10 Hongshiyuan landslide dam (image from Gaofen -1 satellite)

330

As shown in the Fig 10, we can acquire the angle of the riverbed θ and the landslide surface α through analysis of the change of the elevation along the river and the landslide track. As the recording of the repose angle of the debris is missing, the average value of other cases is taken as a rough estimation. And the recording of repose angle φ is missing, it is set as 35.5° , according to the average value of other landslide dam(Wang et al., 2013).

335

Putting the parameters above into the model proposed in 3.3, we can calculate the highest elevation of the dam crest. As it is the lowest elevation of the dam crest that decides the break of dam, formula (9) is

336

337 used to fitting the relationship between the lowest crest and the highest crest. The elevation of the lowest
 338 elevation of the dam crest is 1123.7 m. And the potential maximum volume of the lake can be calculated
 339 easily with the DEM. The comparison of field survey and predicting outcome is shown in Table 2, which
 340 suggests a strong consistency between them.

Parameter	Measured data	The predicting outcome	Error
the lowest elevation of the dam top	1222(m)	1223.7(m)	1.7(m)
the maximum of lake volume	$2.6 \times 10^8 (m^3)^*$	$3.1 \times 10^8 (m^3)$	$0.4 \times 10^8 (m^3)^*$

341 Table 2 predicting outcome and measured data from field survey(Zhou et al., 2015; Luo et al., 2019).
 342
 343

344 5. Discussion

345 5.1. Rapid hazard assessment

346 The lowest height of the dam crest and the maximum volume of the barrier lake are important input
 347 parameters for the dam-breaking model. This paper has given the procedure to obtain them rapidly. We
 348 take Baige landslide dam as an example to illustrate how to use the prediction results to carry out rapidly
 349 hazard assessment.

350 Many scholars have found the correlation between the geometric parameters of landslide dam and its risk
 351 by empirical formula. On the basis of the prediction results and the formulas they provide, we can make
 352 a quick prediction of the key information of the landslide dam hazard, such as the dam volume, the
 353 stability of the barrier dam and the potential maximum discharge of the lake.

354 The width of the barrier dam can be obtained directly from remote sensing images, which is 574.6m.
 355 As the edge and Angle conditions in the simplified model (Fig 4) have been cleared, that is, all the
 356 simplified section plane parameters in the model can be obtained. So based on the relationship between
 357 edges and angles in the model, the distance between top and bottom in the lowest crest, H'_l , and the
 358 length of the dam top, L'_T , can be expressed by the following formula (10), (11).

$$359 \quad H'_l = \cos \theta (0.63H_h + 5.59 - H_r) \quad (10)$$

$$360 \quad L'_T = L'_B - \frac{H'}{\tan \beta_d} - \frac{H'}{\tan \beta_u} \quad (11)$$

361 However, because the cross section of the barrier dam is not evenly distributed in the direction of the

362 vertical river, the height change will occur as discussed in 3.5. We can assume that the change of its top
 363 height is basically linear and the bottom side length and top side length of the section trapezoid do not
 364 change in the direction of the vertical channel. Therefore, we can obtain the estimation Formula (12) to
 365 calculate the volume of the dam debris. In the case of Baige landslide dam, the prediction outcome is
 366 $32.4 \times 10^6 m^3$, and the true value according to field survey is $30.2 \times 10^6 m^3$ (Shen et al., 2020). The
 367 error is mainly induced by the elevation change of riverbed in the direction of the vertical channel., which
 368 has a great influence to area of the dam section when the width of the dam is large.

$$369 \quad V_d = \frac{1}{4} W (H_l' + H_h') (L_B' + L_T') \quad (12)$$

370 In Dong research, a regression model to evaluate the stability of the barrier lake is proposed based on the
 371 case of the historical landslide dam (Dong et al., 2011a), as shown in Formula (13).

$$372 \quad L_s = -2.55 \log(P) - 3.64 \log(H_l) + 2.99 \log(W) + 2.73(L) - 3.87 \quad (13)$$

373 Where P, H_l, W, L are the inflow, dam height, width and length of the landslide dam. In the case of
 374 Baige landslide, the inflow of Baige landslide dam is $822 m^3 / s$ (Li et al., 2019). The result L_s is -
 375 1.472, which means that Baige landslide dam is unstable and has a high risk to breach.

376 In the simple prediction formula (14) proposed by Cenderelli., V is the maximum volume of the dammed
 377 lake, and Q is the maximum flood peak of dam breaching. Without treatment, the largest flood peak of
 378 the Baige Landslide Dam breaching will reach $42257 (m^3 / s)$.

379

$$380 \quad Q = 3.4 \cdot V^{0.46} \quad (14)$$

381 The comparison between the predicted result and the measured date, as shown in table 3, achieves a good
 382 agreement. The rapid assessment of the dam breaching hazard has been completed. As the simulation
 383 model of dam breaching has a significant influence on the prediction of these factors, they should also
 384 be selected carefully in practical applications. Besides formulas above, there are also many other
 385 formulas to choose to complete the prediction (Costa and Schuster, 1991; Walder and OConnor, 1997;
 386 Shi et al., 2014; Ruan et al., 2021; Peng and Zhang, 2012; Zhong et al., 2018; Ermini and Casagli, 2003;
 387 Dong et al., 2011a; Shen et al., 2020). And many scholars have discussed the merits and demerits between
 388 these hazard assessment models (Peng and Zhang, 2012; Fan et al., 2021).

389

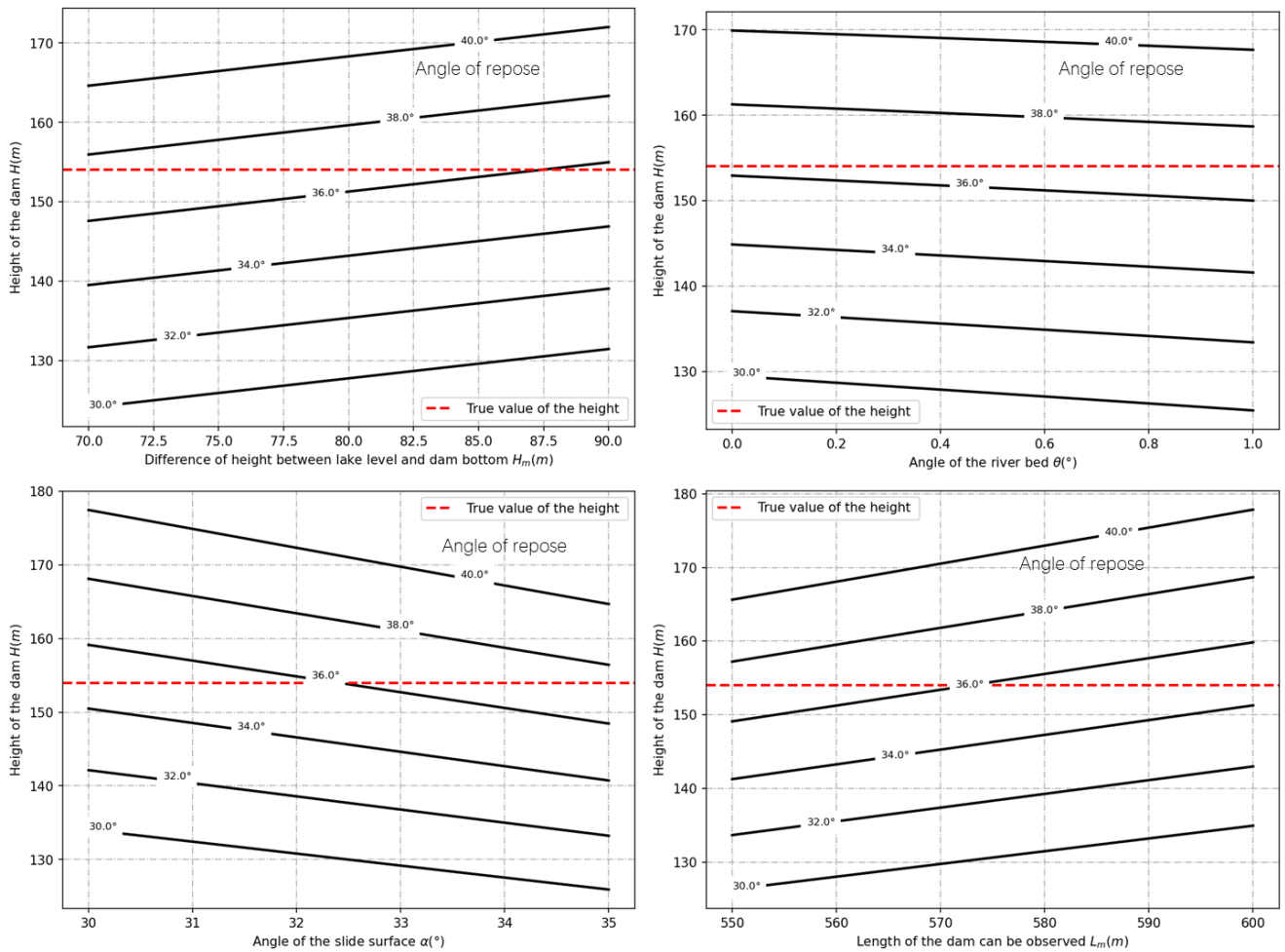
Parameter	Measured data	The predicting outcome
Tthe highest elevation of the dam top	3014 (m)	3016.5(m)
The lowest elevation of the dam top	2967 (m)	2964.2(m)
The maximum of lake volume	$8.69 \times 10^8 (m^3)^*$	$7.96 \times 10^8 (m^3)$

The dam volume	$30.2 \times 10^6 (m^3)$	$32.4 \times 10^6 (m^3)$
The stability of dam	Not stable	Not stable
The peak discharge	$41624 (m^3 / s)^*$	$42257 (m^3 / s)$

390 Table 3 the comparison of the measured data and the predicted result. As relative measures have been
391 taken to reduce the maximum volume of the barrier lake, data with star in the table is the estimation
392 results of Chen’s detailed back analyses(Chen et al., 2020).

393 5.2. Sensitivity analysis

394 In this procedure, the main parameters include: the length of the dam that can be observed, the elevation
395 of the lake level, the elevation of the dam bottom, the slope angle of landslide surface and the inclination
396 angle of the riverbed. Since H_m is the lake level elevation minus the elevation of the dam bottom,
397 sensitivity analysis of these two parameters will be conducted on H_m directly. The variation of the
398 prediction result with the change of parameters is shown as follows:
399



400

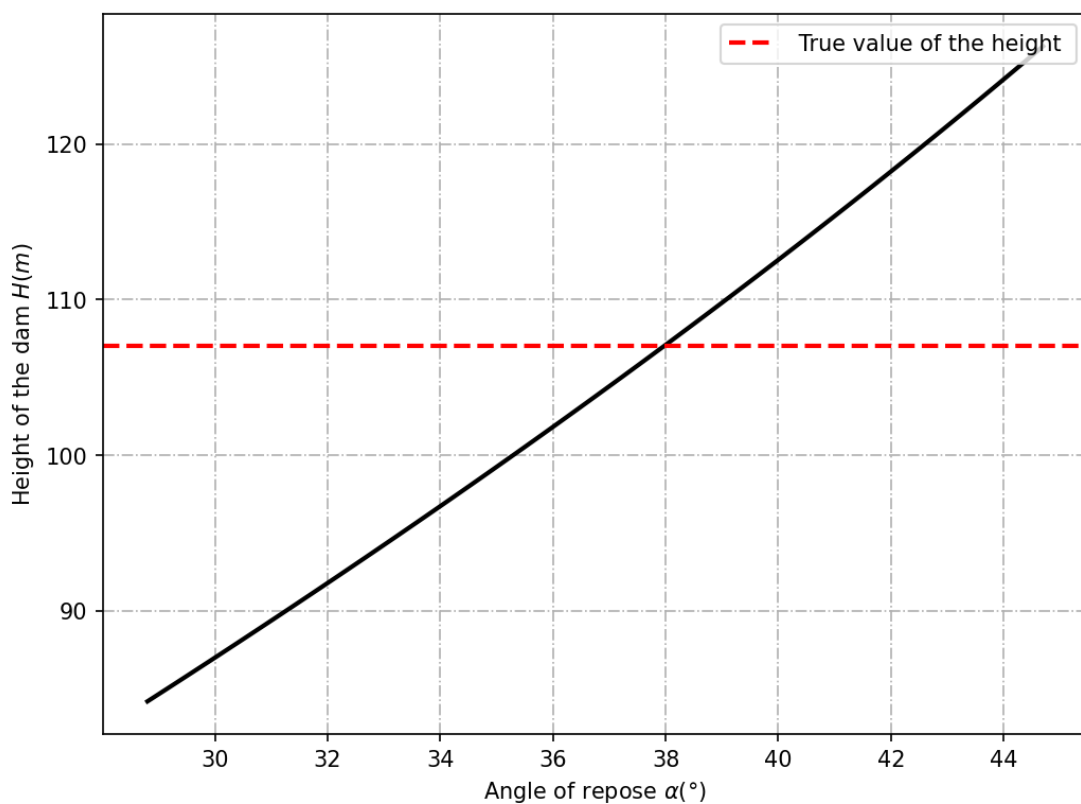
401 Fig 11 the relationship between the predicted result and the input parameters.

402

403 As can be seen from Fig 11, with other parameters unchanged, the greater the observable length of the
404 dam and the difference of height between the lake level and dam bottom, the higher the dam crest. The
405 crest of the dam gets lower as the slope angle of landslide surface and the inclination angle of the riverbed
406 rise. The slope foot of the dam is mainly affected by the angle of landslide surface and inclination angle
407 of the riverbed. The smaller the slope foot, the smaller the height of the dam. The calculated results are
408 in good agreement with expectations.

409 Meantime, it can be found that these parameters all have an impact of about 10% on the final prediction
410 results. So, it is necessary to be careful to determine these parameters. Possible methods to reduce errors
411 include repeat procedures and more reliable historical data.

412



413 Fig 12 the relationship between the predicted result and the angle of repose.

414

415 Finally, it is found that the angle of repose of the dam body has a significant influence on the height of
416 the dam (Fig 12). The greater the angle of repose, the greater the estimate of dam height. According to
417 Wang's field survey, the angle of repose of the landslide dams in Wenchuan earthquake ranges from 28.8°
418 to 44.7°, with an average value of 35.5°(Wang et al., 2013). In the absence of the historical date, the
419 average value proposed by Wang can be used. However, in this way, the difference between the final
420 result and the true value can be about 30% in the worst case. Therefore, on the premise of sufficient
421 disaster relief resources, it is better to make a bad estimate of the repose angle, so as not to make a wrong
422 judgment on the hazard. On the other hand, it is also possible to check the repose angle of the material

423 in advance in landslide prone area, so as to make a quick hazard assessment after the landslide.

424 5.3. Influence of image resolution

425 The remote sensing image used in this research is Beijing-1 with a resolution of 0.8m. The pre-landslide
 426 DEM is SRTM V3 with a resolution of 30m. As more and more remote sensing data are available, in
 427 addition to satellite-based remote sensing platform, small UAV remote sensing platform can also be well
 428 applied to this procedure. As different sensors and remote sensing platforms may have different
 429 resolutions, we use interpolation to obtain images with different resolutions to explore the appropriate
 430 resolution for this procedure (Table 2; Table 3).

431

Resolution	Input						
	H_1 (m)	H_0 (m)	H_m (m)	L_m (m)	α (°)	θ (°)	φ (°)
0.8	2944	2860	84	567	30.65	0.11	35.5
5	2946	2861	70	545	28.58	0.10	35.5
15	2943	2856	73	562	29.44	0.09	35.5
30	2956	2862	84	540	29.10	0.16	35.5

432 Table 4 the parameters obtained through different resolution image, where H_1 is the elevation of the
 433 lake level, H_0 is the elevation of the dam bottom, H_m is H_1 minus H_0 , L_m is the length of the
 434 dam that can be observed in the image, α is the slope angle of landslide surface, θ is the inclination
 435 angle of the riverbed and φ is the angle of repose

Resolution	Output	Accuracy	
	H (m)	True value H (m)	Error(m)
0.8	2964.2	2967	2.8
5	2964.7	2967	2.3
15	2961.6	2967	5.4
30	2960.5	2967	6.5

436 Table 5 the predicted result of image with different resolutions

437 As we discussed before, the main parameters in this procedure include the length of the dam that can be
 438 observed, the lake level, the elevation of the dam bottom, the slope angle of landslide surface and the
 439 inclination angle of the riverbed. Obviously, the resolution of the image will affect all of these five (Table
 440 4), but mainly affect the determining of length of the dam that can be observed and the lake level. In
 441 general, the higher the resolution, the more accurate the prediction results obtained. When the resolution
 442 drops from 0.8m to 30m, the error of prediction results changes from 2.8m to 6.5m, as shown in Table 5.
 443 But for the procedure this paper proposed, image with resolution of 5m is sufficient for a good estimate
 444 of the dam height.

445 There is no doubt that the resolution and quality of DEM data are very important for this procedure.
 446 However, due to the lack of comparative data, this paper does not conduct in-depth discussion on it. For

447 this part, Dong has had relevant discussions in his research(Dong et al., 2014) for readers' reference.

448 5.4. Other discussion

449 In this study, the predicting model ofis mainly based on the formation mechanism of the barrier dam
450 combined with a single remote sensing image and pre-landslide DEM to quickly predict the essential
451 paraments of the landslide dam hazard. Therefore, a more comprehensive assessment of the reliability of
452 formation mechanism has also been carried out. It is found that most laws can be applied well, but
453 formula (3) has greater limitations in fitting the "cut-top" effect. In Wu’s experiment, the “cut-top” effect
454 fitting is mainly determined by the slope angle of landslide surface. Actually, the angle between the
455 riverbed plane and slop surface of the dam should be determined by its landslide potential energy,
456 landslide length, and landslide angle(Grasselli et al., 2000; Xu et al., 2013; Iverson et al., 2015). In
457 addition to the slope angle of landslide surface, the length of the landslide and potential energy are equally
458 important. In Wu's formula, only the slope angle of landslide surface is considered, so more experiments
459 are needed to improve the fitting.

460 As there is not enough theoretical research to support the prediction of the lowest elevation of the dam
461 crest, the method proposed in this paper still has certain limitations. In addition, the mechanism of the
462 relationship between the highest elevation of the dam crest and the lowest elevation of the dam crest is
463 not clear. In most cases, when it comes to the height of a barrier lake, usually only the highest or lowest
464 elevation is recorded, resulting in fewer complete records of both parameters. As the recording in most
465 cases is not completed, only a small number of cases are used to carry out the fitting. Therefore, this
466 aspect still needs more work and related research to support relevant predictions.

467

468 6. Conclusion

469 This research proposes a procedure based on a single remote sensing image to predict the height of the
470 dam crest and rapidly assess the hazard. With the after-landslide remote sensing image, it only takes no
471 more than one human hour to complete the whole procedure. Compared with Dong’s procedure(, this
472 method only requires only one single remote sensing image and has a wider applicability. In view of the
473 large topographic changes in the landslide area, a more reasonable method of using the pre-landslide
474 DEM is proposed. Even the use of poor-quality DEM can complete the relevant prediction and hazard
475 assessment. In the case of Baige Landslide Dam, by extracting the barrier lake surface elevation and
476 determining the bottom elevation of the dam, the prediction of the highest elevation of the dam crest is
477 completed, and the difference between the predicted results and the measured data is within 3m. Since
478 the lowest point of the dam crest determines the potential maximum volume of the barrier lake, we based
479 on historical records find that the height of the highest point and the lowest point of the landslide dam

480 crest basically conforms to the linear relationship. The relationship is expressed as a formula (9) through
481 unary fitting. The prediction result of the lowest elevation of the top of the Baige Landslide Dam is
482 2964.2m, whose error is 2.8m compared to data from field survey, 2967 m. And in the case of Hongshiyan
483 landslide dam, the error of predicting result of dam top elevation is 1.7m.

484

485 In the discussion part, some essential parameters of landslide dam, such as the volume of the dam, the
486 stability of the dam and the potential maximum flood peak of the dam break without treatment, is
487 calculated based on the predicting result, which is basically consistent with the true value. The sensitivity
488 of the parameters used in this method is analyzed, and it is found that the repose angle of the landslide
489 material can affect the prediction result up to 30%. Therefore, the repose angle should be carefully
490 determined when using this procedure for related applications. Finally, through experiment with different
491 resolutions of remote sensing images, we find that as the resolution becomes lower, the accuracy of this
492 method decreases. The resolution of 5m and above is a reasonable range for applying this method,
493 otherwise it will be difficult to distinguish the dam body and the water boundary.

494 **Data availability**

495 The data are available from the authors upon request.

496 **Author Contributions**

497 WJZ designed the experiments, and YZ carried them out. SXW and FTW gave some very important
498 suggestions on basic knowledge of landslide dams. LTW, WLL, ZQ and JFZ helped to operate the whole
499 procedure. QG, ZQW helped with some figures, and YBX provided some remote sensing images. FTW
500 prepared the manuscript with contributions from all co-authors.

501 **Competing interests**

502 The authors declare that they have no conflict of interest.

503 **Acknowledgements**

504 We appreciate the constructive reviews provided by three anonymous reviewers and editor Hans-Balder
505 Havenith. The authors acknowledge the support from the National Key R&D Program of China under
506 Grant 2017YFB0504101 and Grant 2021YFB3901201.

507 **Financial support**

508 This research has been supported by the National Key R&D Program of China under Grant
509 2017YFB0504101 and Grant 2021YFB3901201.

510

511

512

513 **Reference**

514 Adams, J.: Earthquake-dammed lakes in New Zealand, 9, 215–219, 1981.

515 Anon: Exploring machine learning potential for climate change risk assessment, 103752,
516 <https://doi.org/10.1016/j.earscrev.2021.103752>, 2021.

517 Ayalew, L. and Yamagishi, H.: The application of GIS-based logistic regression for landslide
518 susceptibility mapping in the Kakuda-Yahiko Mountains, Central Japan, *Geomorphology*, 65, 15–31,
519 <https://doi.org/10.1016/j.geomorph.2004.06.010>, 2005.

520 Braun, A., Cuomo, S., Petrosino, S., Wang, X., and Zhang, L.: Numerical SPH analysis of debris flow
521 run-out and related river damming scenarios for a local case study in SW China, *Landslides*, 15, 535–
522 550, <https://doi.org/10.1007/s10346-017-0885-9>, 2018.

523 Briaud, J.-L.: Case Histories in Soil and Rock Erosion: Woodrow Wilson Bridge, Brazos River Meander,
524 Normandy Cliffs, and New Orleans Levees, 134, 1425–1447, [https://doi.org/10.1061/\(ASCE\)1090-
525 0241\(2008\)134:10\(1425\)](https://doi.org/10.1061/(ASCE)1090-0241(2008)134:10(1425)), 2008.

526 Canuti, P., Casagli, N., Ermini, L., Fanti, R., and Farina, P.: Landslide activity as a geoinicator in Italy:
527 significance and new perspectives from remote sensing, *Environ. Geol.*, 45, 907–919,
528 <https://doi.org/10.1007/s00254-003-0952-5>, 2004.

529 Cao, Z., Yue, Z., and Pender, G.: Landslide dam failure and flood hydraulics. Part II: coupled
530 mathematical modelling, 59, p.1021-1045, 2011.

531 Chen, C.-Y., Chen, T.-C., Yu, F.-C., and Hung, F.-Y.: A landslide dam breach induced debris flow – a case

- 532 study on downstream hazard areas delineation, *Env Geol*, 47, 91–101, [https://doi.org/10.1007/s00254-](https://doi.org/10.1007/s00254-004-1137-6)
533 004-1137-6, 2004.
- 534 Chen, X. and Lu: *Geomatics-based Method Research on Capacity Calculation of Quake Lake*, 2008.
- 535 Chen, Z., Chen, S., and Wang, L.: Back analysis of the breach flood of the 11.03 Baige barrier lake at the
536 Upper Jinsha River, 2020.
- 537 Chen, Z., Zhou, H., Ye, F., Liu, B., and Fu, W.: The characteristics, induced factors, and formation
538 mechanism of the 2018 Baige landslide in Jinsha River, Southwest China, *Catena*, 203, 105337,
539 <https://doi.org/10.1016/j.catena.2021.105337>, 2021.
- 540 Costa, J. E. and Schuster, R. L.: The formation and failure of natural dams, 100, 1054–1068,
541 [https://doi.org/10.1130/0016-7606\(1988\)100<1054:TFAFON>2.3.CO;2](https://doi.org/10.1130/0016-7606(1988)100<1054:TFAFON>2.3.CO;2), 1988.
- 542 Costa, J. E. and Schuster, R. L.: Documented historical landslide dams from around the world,
543 Documented historical landslide dams from around the world, U.S. Geological Survey, Vancouver, WA,
544 <https://doi.org/10.3133/ofr91239>, 1991.
- 545 Cui, P., Zhu, Y., Han, Y., Chen, X., and Zhuang, J.: The 12 May Wenchuan earthquake-induced landslide
546 lakes: distribution and preliminary risk evaluation, *Landslides*, 6, 209–223,
547 <https://doi.org/10.1007/s10346-009-0160-9>, 2009.
- 548 Dong, J.-J., Tung, Y.-H., Chen, C.-C., Liao, J.-J., and Pan, Y.-W.: Logistic regression model for predicting
549 the failure probability of a landslide dam, *Engineering Geology*, 117, 52–61,
550 <https://doi.org/10.1016/j.enggeo.2010.10.004>, 2011a.
- 551 Dong, J.-J., Tung, Y.-H., Chen, C.-C., Liao, J.-J., and Pan, Y.-W.: Logistic regression model for predicting
552 the failure probability of a landslide dam, *Engineering Geology*, 117, 52–61,
553 <https://doi.org/10.1016/j.enggeo.2010.10.004>, 2011b.
- 554 Dong, J.-J., Lai, P.-J., Chang, C.-P., Yang, S.-H., Yeh, K.-C., Liao, J.-J., and Pan, Y.-W.: Deriving
555 landslide dam geometry from remote sensing images for the rapid assessment of critical parameters
556 related to dam-breach hazards, *Landslides*, 11, 93–105, <https://doi.org/10.1007/s10346-012-0375-z>,
557 2014.
- 558 Ermini, L. and Casagli, N.: Prediction of the behaviour of landslide dams using a geomorphological
559 dimensionless index, 28, 31–47, <https://doi.org/10.1002/esp.424>, 2003.
- 560 Fan, X., van Westen, C. J., Xu, Q., Gorum, T., and Dai, F.: Analysis of landslide dams induced by the
561 2008 Wenchuan earthquake, *Journal of Asian Earth Sciences*, 57, 25–37,
562 <https://doi.org/10.1016/j.jseae.2012.06.002>, 2012.
- 563 Fan, X., Dufresne, A., Siva Subramanian, S., Strom, A., Hermanns, R., Tacconi Stefanelli, C., Hewitt, K.,
564 Yunus, A. P., Dunning, S., Capra, L., Geertsema, M., Miller, B., Casagli, N., Jansen, J. D., and Xu, Q.:
565 The formation and impact of landslide dams – State of the art, *Earth-Science Reviews*, 203, 103116,
566 <https://doi.org/10.1016/j.earscirev.2020.103116>, 2020.
- 567 Fan, X., Dufresne, A., and Whiteley, J.: Recent technological and methodological advances for the
568 investigation of landslide dams, 218, 103646, <https://doi.org/10.1016/j.earscirev.2021.103646>, 2021.
- 569 Grasselli, Y., Herrmann, H. J., Oron, G., and Zapperi, S.: Effect of impact energy on the shape of granular
570 heaps, *GM*, 2, 97–100, <https://doi.org/10.1007/s100350050039>, 2000.
- 571 Han, Y., Chun, Q., and Wang, H.: Quantitative safety evaluation of ancient Chinese timber arch lounge
572 bridges, *Journal of Wood Science*, 68, 4, <https://doi.org/10.1186/s10086-022-02011-y>, 2022.
- 573 Iverson, R. M., George, D. L., Allstadt, K., Reid, M. E., Collins, B. D., Vallance, J. W., Schilling, S. P.,
574 Godt, J. W., Cannon, C. M., and Magirl, C. S.: Landslide mobility and hazards: implications of the 2014

- 575 Oso disaster, 2015.
- 576 Li, H., Qi, S., Chen, H., Liao, H., Cui, Y., and Zhou, J.: Mass movement and formation process analysis
577 of the two sequential landslide dam events in Jinsha River, Southwest China, *Landslides*, 16, 2247–2258,
578 <https://doi.org/10.1007/s10346-019-01254-z>, 2019.
- 579 Li, T. C., Schuster, R. L., and Wu, J. S.: Landslide dams in south-central China, 1986.
- 580 Luo, J., Pei, X., Evans, S. G., and Huang, R.: Mechanics of the earthquake-induced Hongshiyuan landslide
581 in the 2014 Mw 6.2 Ludian earthquake, Yunnan, China, *Engineering Geology*, 251, 197–213,
582 <https://doi.org/10.1016/j.enggeo.2018.11.011>, 2019.
- 583 Meng, C.-K., Chen, K.-T., Niu, Z.-P., Di, B.-F., and Ye, Y.-J.: Influence of Internal Structure on Breaking
584 Process of Short-Lived Landslide Dams, 9, 2021.
- 585 Mora Castro, S.: The 1992 Río Toro landslide dam, Costa Rica, *Landslide News*, 1993.
- 586 Morgenstern, R., Massey, C., Rosser, B., and Archibald, G.: Landslide Dam Hazards: Assessing Their
587 Formation, Failure Modes, Longevity and Downstream Impacts, 2021.
- 588 Peng, M. and Zhang, L. M.: Breaching parameters of landslide dams, *Landslides*, 9, 13–31,
589 <https://doi.org/10.1007/s10346-011-0271-y>, 2012.
- 590 Ruan, H., Chen, H., Wang, T., Chen, J., and Li, H.: Modeling Flood Peak Discharge Caused by
591 Overtopping Failure of a Landslide Dam, 13, 921, <https://doi.org/10.3390/w13070921>, 2021.
- 592 Shen, D., Shi, Z., Peng, M., Zhang, L., and Jiang, M.: Longevity analysis of landslide dams, 17, 2020.
- 593 Shi, Z., Ma, X., and Peng, M.: STATISTICAL ANALYSIS AND EFFICIENT DAM BURST
594 MODELLING OF LANDSLIDE DAMS BASED ON A LARGE-SCALE DATABASE, 33, 1780–1790,
595 2014.
- 596 Walder, J. S. and OConnor, J. E.: Methods for predicting peak discharge of floods caused by failure of
597 natural and constructed earthen dams, *Water Resour. Res.*, 33, 2337–2348,
598 <https://doi.org/10.1029/97WR01616>, 1997.
- 599 Wang, J.-J., Zhao, D., Liang, Y., and Wen, H.-B.: Angle of repose of landslide debris deposits induced
600 by 2008 Sichuan Earthquake, *Eng. Geol.*, 156, 103–110, <https://doi.org/10.1016/j.enggeo.2013.01.021>,
601 2013.
- 602 Wang, Z. H. and Lu, J. T.: Satellite monitoring of the Yigong landslide in Tibet, China, in: *Earth
603 Observing Systems VII*, Bellingham, 34–38, <https://doi.org/10.1117/12.453739>, 2002.
- 604 Wu, H., Nian, T., Chen, G., Zhao, W., and Li, D.: Laboratory-scale investigation of the 3-D geometry of
605 landslide dams in a U-shaped valley, *Engineering Geology*, 265, 105428,
606 <https://doi.org/10.1016/j.enggeo.2019.105428>, 2020.
- 607 Xu, W.-J., Xu, Q., and Wang, Y.-J.: The mechanism of high-speed motion and damming of the
608 Tangjiashan landslide, *Eng. Geol.*, 157, 8–20, <https://doi.org/10.1016/j.enggeo.2013.01.020>, 2013.
- 609 Yang, S.-H., Pan, Y.-W., Dong, J.-J., Yeh, K.-C., and Liao, J.-J.: A systematic approach for the assessment
610 of flooding hazard and risk associated with a landslide dam, *Nat Hazards*, 65, 41–62,
611 <https://doi.org/10.1007/s11069-012-0344-9>, 2013.
- 612 Yunjian, G., Siyuan, Z., Jianhui, D., Zhiqiu, Y., and Mahfuzur, R.: Flood assessment and early warning
613 of the reoccurrence of river blockage at the Baige landslide, *J. Geogr. Sci.*, 31, 1694–1712,
614 <https://doi.org/10.1007/s11442-021-1918-9>, 2021.
- 615 Zhang, L., Xiao, T., He, J., and Chen, C.: Erosion-based analysis of breaching of Baige landslide dams

- 616 on the Jinsha River, China, in 2018, 2019.
- 617 Zhong, Q. M., Chen, S. S., Mei, S. A., and Cao, W.: Numerical simulation of landslide dam breaching
618 due to overtopping, *Landslides*, 15, 1183–1192, <https://doi.org/10.1007/s10346-017-0935-3>, 2018.
- 619 Zhou, J., Cui, P., and Hao, M.: Comprehensive analyses of the initiation and entrainment processes of
620 the 2000 Yigong catastrophic landslide in Tibet, China, *Landslides*, 13, 39–54,
621 <https://doi.org/10.1007/s10346-014-0553-2>, 2016.
- 622 Zhou, X., Chen, Z., Yu, S., Wang, L., Deng, G., Sha, P., and Li, S.: Risk analysis and emergency actions
623 for Hongshiyuan barrier lake, *Nat Hazards*, 79, 1933–1959, <https://doi.org/10.1007/s11069-015-1940-2>,
624 2015.
- 625